ARTICLE IN PRESS

Available online at www.sciencedirect.com
SCIENCE DIRECT®

Journal of Process Control xxx (2005) xxx–xxx

JOURNAL OF PROCESS CONTROL

www.elsevier.com/locate/jprocont

A flexible nonlinear model predictive control scheme for quality/performance handling in nonlinear SMB chromatography

Mazen Alamir [a,*], Fadi Ibrahim [a], Jean Pierre Corriou [b]

[a] *Laboratoire d'Automatique de Grenoble, CNRS/INPG/UJF, BP 46, Domaine Universitaire, 38400 Saint Martin d'Hères, France*
[b] *Laboratoire des Sciences du Génie-Chimique, Groupe ENSIC, 1, rue Grandville, BP 451, 54001 Nancy Cedex, France*

Received 23 June 2004; received in revised form 16 June 2005; accepted 4 July 2005

Abstract

In this paper, a new state feedback scheme is proposed for the control of simulated moving beds with strongly nonlinear isotherms. The proposed scheme offers a unified framework enabling different performance criteria to be improved according to the active production constraints (achieving low cost, improving efficiency, respecting deadlines) that may unpredictably change during the production batch. The proposed scheme is illustrated through several examples showing the robustness of the closed-loop behavior against parameter uncertainties as well as its reactivity to changes in the active auxiliary criterion.

Keywords: Simulated moving bed; Chromatography; Nonlinear constrained model predictive control; Robustness

1. Introduction

Among different separation tools, chromatographic processes gain increasing importance in domains such as food, fine chemicals and pharmaceutical industry where high purities and yields are required. The chromatographic separation principle lies on the different adsorption affinities of the components in a multi-component mixture. Originally, the processes were operated in batch mode and this operation was repeated resulting in a periodic process. Nowadays, the attractive character of continuous processes is realized in the true counter-current chromatographic process where several chromatographic columns are disposed in series in which the solid and liquid phases move in opposite directions. Practically, this continuous process suffers from several drawbacks including in particular the fast degradation of the solid adsorbent, so that it is preferable to simulate its movement by cyclic switching of the inlet and outlet ports in the direction of the fluid flow. Due to its hybrid character including continuous and discrete dynamics, its operational conditions close to the optimum, its great sensitivity to operation parameters and disturbances, the control of the simulated moving bed (SMB) process is complicated and many different strategies have been proposed. In the following, a quick overview of existing solutions is made in order to properly underline the novelty of the feedback methodology proposed in the present paper.

In [1], a simple feedback scheme is proposed that combines PI controller with nonlinear wave propagation module. The idea is to use decoupled PI controllers in order to induce slight movements of the wave fronts once a convenient and optimized cyclic regime is established. The latter is calculated using the Triangle Theory approach that neglects columns efficiency effects. The wave front propagation block uses simple rules that are valid for the equivalent true moving bed. The scheme is dedicated to a maximum feed throughput and minimum solvent consumption operations. It is

* Corresponding author. Tel.: +33 476826326; fax: +33 476826388.
E-mail address: mazen.alamir@inpg.fr (M. Alamir).

0959-1524/$ - see front matter © 2005 Elsevier Ltd. All rights reserved.
doi:10.1016/j.jprocont.2005.07.001

particularly suitable in the absence of precise model of the process.

In [2], an asymptotically input/output linearizing controller is proposed. Both the observer scheme and the input/output linearizing feedback are computed using the equivalent true moving bed.

In [3], a model predictive control is proposed based on the linearized equations. This leads to a LP optimization problem. A linear form of the efficiency cost function is used by taking $F = \lambda_1 Q_D - \lambda_2 Q_F$ as penalty function. The robustness of the proposed scheme has been tested under various uncertainty and disturbance conditions. The two stage philosophy consisting in first achieving purity requirements and then improving auxiliary cost function is also used in the present paper. With this respect, the present paper may be viewed as a generalization of [3] to the case of higher order on-line approximation of the SMB nonlinear model.

Quite similarly, a repetitive model predictive control scheme is proposed in [4] which exploits the periodic nature of the problem. Thus a run-to-run discrete linear model is obtained around some reference configuration by assuming a constant switching period. This model is then used in a MPC scheme in order to maximize the yields under purity-related inequality constraints.

In [5], a two stage feedback control is proposed in which the on-line control task is to maintain the system state regulated along an off-line computed optimal trajectory. In the resulting linear system model, the state and the control are deviations from the off-line computed ones. Recently, a nonlinear model predictive control scheme has been applied to low purity separation process [6].

The feedback scheme proposed in this paper shows the following features:

- The control scheme needs no initially optimized configuration to be available. This can be crucial when unpredictable changes occur in the system configuration (changes in feed composition, desired purities). However, any a priori knowledge on the optimal operation conditions can be easily incorporated by suitably initializing the algorithm.
- The fact that control schemes are often based on off-line computed optimal configuration comes from the fact (see [5]) that the underlying constrained non convex optimal control problem cannot be exactly solved on-line in a classical nonlinear predictive control scheme [7]. To overcome this difficulty, the optimal control problem is solved here during the system life time in the sense that the iterations leading to its solution are distributed in time.
- The feedback scheme handles in a quite flexible and easy way sudden changes in the production planning. This may arise for instance when further to an unpredictable new order, it becomes advantageous to finish the current production earlier than initially decided, including doing this by increasing the desorbent flow rate Q_D that one generally aims to minimize. In such a case, the classical efficiency related cost functions becomes (at least temporarily) irrelevant and may be supplanted by a maximum flow rate cost function that expresses the need to accelerate the production rate whatever is the related cost that is lower than the delay penalty-related cost.
- Apart from [2], few papers consider the yields on the optimization cost function used to update the control variables. The cost function is defined in terms of flow rate dependent function under purity-related inequality constraints. In the feedback scheme proposed in the present paper, the yield is explicitly used in the cost function via a small weight term that is added to the purity constraint violation term.
- The feedback scheme incorporates an integration-like feature to robustify the closed-loop against unavoidable parameter uncertainties.
- The switching time that is frequently taken constant in many existing schemes is a decision variable in the proposed one. This is a crucial feature when several auxiliary performance indexes may be used according to the production context since it enables the quasi invariance of solutions up to a time scaling to be extensively used (see Section 6 for simulations illustrating this feature).

More generally, it goes without saying that the "*best*" control strategy deeply depends on the context. This includes several facts, among other:

- The accuracy of the available model. This depends on the initial knowledge on the system's parameters as well as whether an on-line parameter estimation is being used. Such estimation may be done through on-line nonlinear least squares minimization. This is made easier by the fact that the limit cycles are initial state independent. This enables to decouple the effect of modelling error and initial state estimation errors.
- The uncertainties on the production scheduling that determine to which extent the performance index may vary. This is also linked to the quality of the feed stream as well as that of the local flow rate regulation and measurement systems.
- The amplitude of the set point changes that may disqualify linearization based schemes as well as the degree of desired purity that render the strategies based on the use of equivalent true moving bed inappropriate.

The paper is organized as follows: First some facts on simulated moving bed (SMB) chromatography are recalled in Section 2. The control problem is stated in Section 3. Some definitions and notations are given in

Section 4. The proposed feedback algorithm is given in Section 5 while illustrative scenario are proposed in Section 6 to assess the efficiency and underline some features of the proposed feedback scheme.

2. Recalls on binary simulated moving beds

Simulated moving bed (SMB) is a continuous countercurrent separation process in which the movement of the solid phase is simulated by switching the inlet/outlet ports in the liquid flow direction (Fig. 1). The process is obtained by connecting in series several single chromatographic columns to form four functional sections. Fig. 1 shows a SMB with five columns per section. Each of these sections is defined by its boundary ports. For instance, Section 1 is the one between the desorbent inlet and the extract outlet. Since these ports switch, the functional sections are geometrically moving.

Because of their different adsorption affinities, the two components initially present in the feed inlet have different equivalent convection velocities through the sections. This results in the less adsorbed component being extracted at the raffinate outlet while the more adsorbed component is recovered at the extract outlet.

The performances of the SMB can be monitored by five independent variables. These are the delay $\tau_s > 0$ between switches and four independent flow rates that are chosen here to be Q_D, Q_{ext}, Q_F and Q_{IV}. The remaining flow rates may be computed by simple mass balance equations under liquid incompressibility assumption.

In what follows, U denotes these decision variables

$$U := (Q_D \; Q_{ext} \; Q_F \; Q_{IV} \; \tau_s)^T \in \mathbb{U} \tag{1}$$

where $\mathbb{U}$ denotes the compact set of possible values for which all the flow rates are positive and lower than their saturation levels, this reduces to the following constraints:

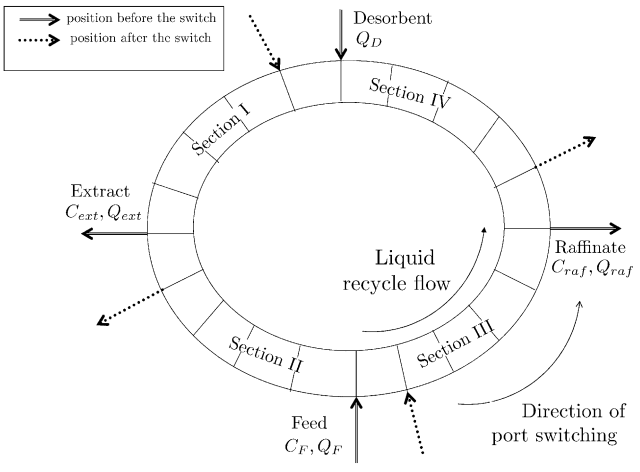

Fig. 1. Schematic view of a simulated moving bed.

$$\forall i \in \{1,\ldots,5\}, \quad U_i^{\min} \leqslant U_i \leqslant U_i^{\max} \tag{2}$$

$$U_2 \leqslant U_1 + \min\{U_3, U_4\} \tag{3}$$

Considering a binary SMB with n_c columns, the state vector $C \in \mathbb{R}_+^{2n_c}$ is obtained by concatenating $C_a \in \mathbb{R}_+^{n_c}$ and $C_b \in \mathbb{R}_+^{n_c}$ where $C_{a,i}$ [respectively $C_{b,i}$] is the concentration of species (a) [respectively (b)] in the ith column. Since the system's equations depend on the positions of the ports; let $\sigma \in \{1,\ldots,n_c\}$ be the configuration index, say, the position of the Feed inlet for instance. The evolution of σ is piecewise constant with jumps occurring at the switching instants t_k, that is

$$\sigma(t_k + \tau_s(t_k)) = \sigma(t_k)\mathrm{mod}(n_c) + 1$$

and assuming instantaneously reachable equilibrium between liquid and solid phases, the system equations under piecewise constant control $U(\cdot)$, that is, a control being constant between two successive switches, may be written as follows:

$$\dot{C}(t) = F_{\sigma(t_k)}(C(t), U(t_k), C_F(t)) \quad t \in [t_k, t_{k+1}[\tag{4}$$

$$\sigma(t_k + U_5(t_k)) = \sigma(t_k)\mathrm{mod}(n_c) + 1 \tag{5}$$

where $F_\sigma(\cdot)$ is the smooth convection–diffusion evolution law that holds under the configuration σ.

It is worth noting that the control algorithm proposed in this paper is valid for any "simulation model" that may be used to predict the behavior of the SMB under some control. The simplifications leading to (4), (5) are not mandatory. If more detailed simulation model is available, it can be used.

On the other hand, the control strategy proposed in the following assumes the state to be completely measured. It goes without saying that a convenient state observer [8–11] has to be used.

3. The control problem

Assume that the SMB operates over $[t_0, t_0 + T]$ to satisfy a customer's order. Denote by m_a^{ext} and m_a^{raf} [respectively m_b^{ext} and m_b^{raf}] the mass of species (a) [respectively (b)] collected at the extract and the raffinate ports over the operating interval $[t_0, t_0 + T]$. One clearly has

$$m_j^{ext} = \int_{t_0}^{t_0+T} Q_{ext}(t) \cdot C_j^{ext}(t)\,dt, \quad j \in \{a, b\}$$

$$m_j^{raf} = \int_{t_0}^{t_0+T} Q_{raf}(t) \cdot C_j^{raf}(t)\,dt, \quad j \in \{a, b\}$$

therefore, in order to keep up with the order's requirements, the following constraints have to be carefully observed.

(1) The purity requirements:

$$\min\left\{\frac{m_a^{ext}}{m_a^{ext} + m_b^{ext}} - p_{ext}^d, \frac{m_b^{raf}}{m_a^{raf} + m_b^{raf}} - p_{raf}^d\right\} \geqslant 0 \tag{6}$$

where $p^{\mathrm{d}}_{\mathrm{ext}}$ and $p^{\mathrm{d}}_{\mathrm{raf}}$ are the contractually minimal purities to hold in the delivered product.

(2) The total produced quantities:

$$m^{\mathrm{ext}}_{\mathrm{a}} \geqslant m^{\mathrm{d}}_{\mathrm{ext}}, \quad m^{\mathrm{raf}}_{\mathrm{b}} \geqslant m^{\mathrm{d}}_{\mathrm{raf}} \tag{7}$$

(3) The delivery deadline: $t_0 + T \leqslant t^{\mathrm{d}}$

an optimal admissible strategy is therefore a one that meets the above requirements while minimizing some cost function. This may be for instance the quantity of desorbent being used, namely

$$J_{\mathrm{D}} := \int_{t_0}^{t_0+T} Q_{\mathrm{D}}(t)\,\mathrm{d}t \tag{8}$$

alternatively, the following efficiency criterion may be used when only one product is of interest

$$J_{\mathrm{E}} := \int_{t_0}^{t_0+T} \frac{Q_{\mathrm{D}}(t)}{Q_i(t)}\,\mathrm{d}t, \quad i \in \{\mathrm{ext}, \mathrm{raf}\} \tag{9}$$

or (when the two products are required)

$$J_{\mathrm{E}} := \int_{t_0}^{t_0+T} \frac{Q_{\mathrm{D}}(t)}{Q_{\mathrm{F}}(t)}\,\mathrm{d}t \tag{10}$$

Finally, when the production rate is to be maximized in order to meet the delivery time constraint, the following criterion maybe used

$$J_{\mathrm{P}} := -\int_{t}^{t+T} [Q_{\mathrm{D}} + Q_{\mathrm{F}}]\,\mathrm{d}\tau \tag{11}$$

provided that the concentration in the outlet flows are taken into account adequately (see below).

Given the initial state $C(t_0)$, the above problem may be considered as a constrained free final-time optimal control problem that can be solved using nonlinear dynamic programming. However, as mentioned in [5], the associated computation complexity would be incompatible with on-line solution in a classical nonlinear predictive control scheme.

4. Some definitions and notations

In order to properly define the feedback strategy, the following definitions are needed:

Definition 1 (*Steady mean solutions*). Given a constant profile $U(\cdot) \equiv U^0$, the corresponding steady mean solution is denoted by $\overline{C}(U^0)$, namely

$$\overline{C}(U^0) := \lim_{t\to\infty} \frac{1}{U^0_5} \int_t^{t+U^0_5} C(\tau)|_{U(\cdot)=U^0}\,\mathrm{d}\tau \tag{12}$$

(Recall that according to (1), U^0_5 is the corresponding constant switching period).

Definition 2 (*Admissible constant profiles*). Given some positive real $\eta > 0$, $U^0 \in \mathbb{U}$ is said to be η-admissible iff the following holds

$$\psi_{\mathrm{ext}}(U^0) := \frac{\overline{C}^{\mathrm{ext}}_{\mathrm{a}}(U^0)}{\overline{C}^{\mathrm{ext}}_{\mathrm{a}}(U^0) + \overline{C}^{\mathrm{ext}}_{\mathrm{b}}(U^0)} - p^{\mathrm{d}}_{\mathrm{ext}} \geqslant \eta \tag{13}$$

$$\psi_{\mathrm{raf}}(U^0) := \frac{\overline{C}^{\mathrm{raf}}_{\mathrm{b}}(U^0)}{\overline{C}^{\mathrm{raf}}_{\mathrm{a}}(U^0) + \overline{C}^{\mathrm{raf}}_{\mathrm{b}}(U^0)} - p^{\mathrm{d}}_{\mathrm{raf}} \geqslant \eta \tag{14}$$

where $p^{\mathrm{d}}_{\mathrm{ext}}$ and $p^{\mathrm{d}}_{\mathrm{raf}}$ are the desired purities. The admissible set defined above is hereafter denoted by $\mathscr{U}_\eta \subset \mathbb{U}$.

The relevance of the above definitions comes from the fact that an admissible profile U^0 makes the purity and the production requirements (6) and (7) achievable in finite time. Roughly speaking, the purity margin $\eta > 0$ is used to compensate for potential "*lack of purity*" that would have been accumulated during the transient phase.

Hereafter, the constraints (13) and (14) are shortly written as follows:

$$J_{\mathrm{pur}}(U^0, \eta) \leqslant 0 \tag{15}$$

where J_{pur} is given by

$$J_{\mathrm{pur}}(U, \eta) := \eta - \min\{\psi_{\mathrm{ext}}(U), \psi_{\mathrm{raf}}(U)\} \tag{16}$$

and the admissibility set can be defined equivalently as follows:

$$\mathscr{U}_\eta := \{U \in \mathbb{U} \quad \text{s.t. } J_{\mathrm{pur}}(U, \eta) \leqslant 0\} \tag{17}$$

When the cost function $J_{\mathrm{pur}}(U,\eta)$ becomes negative, it only guarantees that under the constant profile U, the purities meet the requirement after some finite time, nothing is said about the in-between transient behavior. This is handled by the following definition:

Definition 3 (*Invariant admissible configuration*). The set of invariant admissible configurations $\mathscr{A}^{\mathrm{ad}}_\eta$ is the set of all pairs $(C, U) \in \mathbb{R}^{2n_{\mathrm{c}}} \times \mathscr{U}_\eta$ of initial states C and an admissible constant profiles U such that for all $t \in [0, \infty]$:

$$\frac{\int_t^{t+U_5} C^{\mathrm{ext}}_{\mathrm{a}}(\tau; C; U)\,\mathrm{d}\tau}{\int_t^{t+U_5} \left[C^{\mathrm{ext}}_{\mathrm{a}}(\tau; C; U) + C^{\mathrm{ext}}_{\mathrm{b}}(\tau; C; U)\right]\mathrm{d}\tau} - p^{\mathrm{d}}_{\mathrm{ext}} \geqslant \eta \tag{18}$$

$$\frac{\int_t^{t+U_5} C^{\mathrm{raf}}_{\mathrm{b}}(\tau; C; U)\,\mathrm{d}\tau}{\int_t^{t+U_5} \left[C^{\mathrm{raf}}_{\mathrm{a}}(\tau; C; U) + C^{\mathrm{raf}}_{\mathrm{b}}(\tau; C; U)\right]\mathrm{d}\tau} - p^{\mathrm{d}}_{\mathrm{raf}} \geqslant \eta \tag{19}$$

where $C(\tau; C; U)$ is the solution at instant τ starting at $t = 0$ with the initial state C.

Roughly speaking, when $(C, U) \in \mathscr{A}^{\mathrm{ad}}_\eta$ then by applying the constant profile U, the resulting behavior satisfies the purity requirement over "*all the future*". With this respect, the following cost function is relevant

$$J^{\mathrm{inv}}_{\mathrm{pur}}(C, U, \eta, T) := \min_{t\in[0,T]} [\eta - \min\{\Phi_{\mathrm{ext}}(t), \Phi_{\mathrm{raf}}(t)\}] \tag{20}$$

where Φ_{ext} and Φ_{raf} are the lhs of (18) and (19) respectively. Note that for sufficiently high T, the cost function $J^{\mathrm{inv}}_{\mathrm{pur}}$ pur may be used to characterize the invariant admissible profiles set $\mathscr{A}^{\mathrm{ad}}_\eta$ as follows:

$$\left\{(C,U)\in A_\eta^{\mathrm{ad}}\right\}\Longleftrightarrow\left\{J_{\mathrm{pur}}^{\mathrm{inv}}(C,U,\eta,T)\geqslant 0\right\} \tag{21}$$

this results from the open-loop stability of the mean behavior over switching periods. Namely, if (21) holds for some sufficiently high T, it would be satisfied for all greater T's.

In the above optimization arguments, the concentrations of the components at the extract and the raffinate ports are still not taken into account. Only the purities and the flow rates are used in the definition of the optimization cost. In order to overcome this drawback, the cost functions J_{pur} and $J_{\mathrm{pur}}^{\mathrm{inv}}$ respectively defined by (16) and (20) are redefined as follows:

$$J_{\mathrm{pur}}(U,\eta):=\eta-\min\{\psi_{\mathrm{ext}}(U),\psi_{\mathrm{raf}}(U)\}-\frac{\eta}{2C_{\mathrm{F}}}\min\{\overline{C}_{\mathrm{a}}^{\mathrm{ext}}(U),\overline{C}_{\mathrm{b}}^{\mathrm{raf}}(U)\} \tag{22}$$

$$J_{\mathrm{pur}}^{\mathrm{inv}}(C,U,\eta,T):=\min_{t\in[0,T]}\left[\eta-\min\{\Phi_{\mathrm{ext}}(t),\Phi_{\mathrm{raf}}(t)\}-\frac{\eta}{2C_{\mathrm{F}}}\min\left\{\int_t^{t+T}C_{\mathrm{a}}^{\mathrm{ext}}(\tau)\,\mathrm{d}\tau,\int_t^{t+T}C_{\mathrm{b}}^{\mathrm{raf}}(\tau)\,\mathrm{d}\tau\right\}\right] \tag{23}$$

Indeed, if the optimal values of the original versions (16)–(20) of J_{pur} and $J_{\mathrm{pur}}^{\mathrm{inv}}$ are negative then the optimal values of the new versions (22) and (23) are lower than $\eta/2$ and therefore the purity requirements are still satisfied with a lower margin $\eta/2$ instead of η. Note that C_{F} is constant in our case and is used in (22) and (23) only as a normalization factor.

Assuming an η-admissible constant profile U^0 and an initial profile C^0, the time necessary for the quality and the production requirement (6) and (7) to be achieved is hereafter denoted by

$$\Delta T_{\mathrm{ach}}(C^0,U^0)$$

This enables the set of constant profiles that are compatible with the deadline to be defined:

Definition 4 (*Deadline-compatible constant profiles*). Given a deadline t^{d}, for all $t\in[t_0,t_{\mathrm{d}}[$ and all $\eta>0$, a deadline-compatible constant profile is an admissible constant profile that meets the delivery deadline, namely:

$$\mathscr{U}_{\mathrm{d}}(t,\eta):=\left\{U\in\mathscr{U}_\eta\,|\,t+\Delta T_{\mathrm{ach}}(C(t),U)\leqslant t^{\mathrm{d}}\right\} \tag{24}$$

Finally, the following definition is needed

Definition 5. For all $U\in\mathbb{U}$, the following control transformation

$$\widetilde{U}=\Gamma_\rho(U)\leftrightarrow\begin{cases}\widetilde{U}_i=\rho U_i, & i\in\{1,\ldots,4\}\\ \widetilde{U}_5=U_5/\rho\end{cases} \tag{25}$$

is defined for all $\rho>0$ satisfying

$$\rho\in\left[\frac{U_i^{\min}}{\min_{1\leqslant i\leqslant 4}(U_i)},\frac{U_i^{\max}}{\max_{1\leqslant i\leqslant 4}(U_i)}\right] \tag{26}$$

The transformation (25) is inspired by the fact that in the absence of diffusion, U and $\Gamma_\rho(U)$ leads to the same solution in terms of concentrations up to a time scaling. Typically, such transformation is used to rapidly improve the cost function J_{D} and J_{P} defined above [see (8) and (11)] while leaving quasi invariant the cost function J_{E} [see (10)]. The constraint (26) guarantees that $\Gamma(U)$ still meet the constraint (2) whenever U does.

5. The proposed feedback scheme

The feedback algorithm may be described as follows:

(1) Initial data.
The instant $t=0$ is the starting instant for the production corresponding to an order defined by the quality parameters $p_{\mathrm{ext}}^{\mathrm{d}}$ and $p_{\mathrm{raf}}^{\mathrm{d}}$, the total quantities to be produced $m_{\mathrm{ext}}^{\mathrm{d}}$ and $m_{\mathrm{raf}}^{\mathrm{d}}$ and the delivery deadline t^{d}. Let some security margin $\eta_0>0$ be fixed as well as some initial constant control profile $U(\cdot)=U^0$. Put the switching period index $k=0$ and the initial switching instant $t_k=t_0=0$. Put $i=1$.

(2) During the switching period $[t_k,t_k+U_5^k[$.
The switching time being given by U_5^k, the constant flow rates $U(\cdot)\equiv U_{1,\ldots,4}^k$ are applied over the switching period $[t_k,t_{k+1}:=t_k+U_5^k[$. During this switching period, computations are done to find the control profile to be applied during the next switching period $[t_{k+1},t_{k+1}+U_5^{k+1}]$. In order to do this, a prediction $\widehat{C}(t_{k+1})$ is first computed by simulating the model starting from $C(t_k)$ under the constant control $U_{1,\ldots,4}^k$.

Two main situations are to be distinguished for which, different classes of updating policies are adopted:

(a) $(C(t_k),U^k)\notin\mathscr{A}_\eta^{\mathrm{ad}}$:
In this case, the system has not yet reached an invariant admissible configuration. Therefore, U^k is improved in the sense of decreasing J_{pur} [see (16)–(22)]. Consequently, U^{k+1} is obtained by performing a given number of steps of some minimization subroutine starting from U^k as initial guess. This can be formally written as follows:
Make N iterations

$$(\alpha_i^{(k+1)},U^{k+1})\leftarrow\mathrm{Improve}(J_{\mathrm{pur}},U^k,\alpha_i^{(k)},i) \tag{27}$$

$$i\leftarrow(i\bmod 5)+1 \tag{28}$$

end
where i is the index of the component of U being updated while α_i is the corresponding trust region parameter (more about this is developed in Section 5.2). N is the number of iterations compatible with the available computation time (the switching

period duration).Note that since J_{pur} cannot be indefinitely improved, the control profile becomes constant after a finite number of iterations and since the system is open-loop stable, an invariant admissible configuration is reached (provided that the purity requirements are achievable). The situation (b) hereafter is then "*fired*".

(b) $(C(t_k), U^k) \in \mathscr{A}_\eta^{\text{ad}}$:
In this case, an admissible configuration is reached that is invariant under U^k. However, better control profiles may improve the production cost, the efficiency or the possible delivery time. The choice of the cost function to be considered depends on the context. However, regardless of the context, the principle is the following:The decision variables are split into two categories, namely

$$U := \underset{i\in I_{\text{p}}\cup I_{\text{a}}}{\otimes} U_i; \quad I_{\text{p}}, I_{\text{a}} \subset \{1,\ldots,5\} \tag{29}$$

where I_{p} and I_{a} form a partition of $\{1,\ldots,5\}$. Roughly speaking, I_{p} is the set of indexes of decision variables that are used to create purity margin (the subscript 'p' in I_{p}) by minimizing $J_{\text{pur}}^{\text{inv}}$. This margin enables the other decision variables, called the auxiliary optimizing variables (the subscript 'a' in I_{a}) to decrease some auxiliary function J_{a}, for instance J_{D}, J_{E} or J_{P} defined above (see Fig. 2 for a schematic view of this feature).

More precisely, two situations may occur

(i) Either $U^k \in \mathscr{U}_{\text{d}}(t_k, \eta)$ in which case, the delivery deadline can be respected, therefore, auxiliary optimization may be focused on production cost. This is done hereafter by taking

$$J_{\text{a}} := Q_{\text{D}}, \quad \underset{i\in I_{\text{a}}}{\otimes} U_i = Q_{\text{D}} \quad (I_{\text{a}} := \{1\}) \tag{30}$$

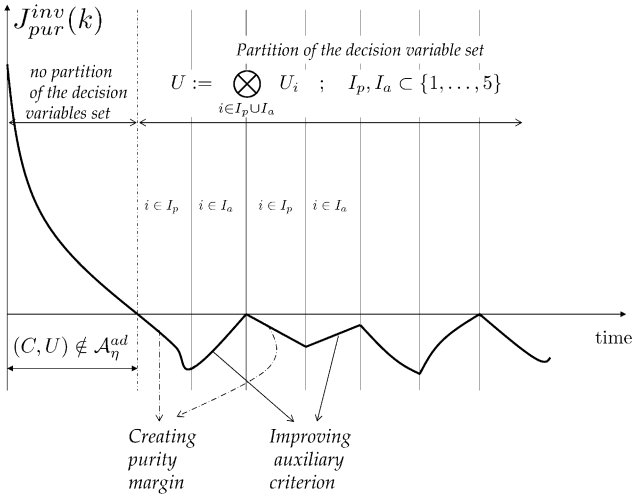

Fig. 2. Schematic view of the control algorithm.

Alternatively, one may be interested in maximizing efficiency by taking

$$J_{\text{a}} := \frac{Q_{\text{D}}}{Q_{\text{F}}}, \quad \underset{i\in I_{\text{a}}}{\otimes} U_i = (Q_{\text{D}}, Q_{\text{F}})^{\text{T}} \quad (I_{\text{a}} := \{1,3\}) \tag{31}$$

equivalent straightforward definitions may be easily derived for the case where efficiency is defined by $Q_{\text{D}}/Q_{\text{raf}}$ or $Q_{\text{D}}/Q_{\text{ext}}$.

(ii) Or $U^k \notin \mathscr{U}_d(t_k, \eta)$ in which case cost consideration is temporarily dropped in favor of maximizing the production rate. In this case, one takes

$$J_{\text{a}} := -(Q_{\text{D}} + Q_{\text{F}})$$

$$\underset{i\in I_{\text{a}}}{\otimes} U_i = (Q_{\text{D}}\ Q_{\text{F}})^{\text{T}}, \quad I_{\text{a}} := \{1,3\} \tag{32}$$

The computations to be performed when $(C(t_k), U^k) \in \mathscr{A}_\eta^{\text{ad}}$ can now be given as follows:Make N iterations

$$(\alpha_i^{(k+1)}, U^{k+1}) \leftarrow \text{Improve}(J^{(i)}, U^k, \alpha_i^{(k)}, i) \tag{33}$$

$$\text{under the constraint} (C(t_{k+1}), U^{k+1}) \in \mathscr{A}_\eta^{\text{ad}} \tag{34}$$

$$\text{and } U^{k+1} \in \mathscr{U}_{\text{d}}(t_{k+1}, \eta) \text{ if } U^k \in \mathscr{U}_{\text{d}}(t_k, \eta) \tag{35}$$

Apply $U^{k+1} \leftarrow \Gamma_\rho(U^{k+1})$ when appropriate by computing a convenient ρ satisfying (26)
$i \leftarrow (i \bmod 5) + 1$
end
where

$$J^{(i)} := \begin{cases} J_{\text{a}} & \text{if } i \in I_{\text{a}} \\ J_{\text{pur}}^{\text{inv}} & \text{otherwise} \end{cases} \tag{36}$$

where J_{a} is given by either (30), (31) or (32) according to the context. Note that the optimization step in (33) is performed under the constraints (34) and (35). In other words, the auxiliary optimization must keep guaranteed all already guaranteed achievements. This is clearly always feasible since keeping the past values is always a candidate option.

A schematic view of the control philosophy is depicted on Fig. 2. Namely, at a first stage ($(C(t_k), U^k) \notin \mathscr{A}_\eta^{\text{ad}}$), no partition of the decision variables is made and all of them are used to decrease the cost function J_{pur}. This is the case (a) of the present section. As soon as $J_{\text{pur}}^{\text{inv}}$ becomes negative ($(C(t_k), U^k) \in \mathscr{A}_\eta^{\text{ad}}$ the case (b) is "*fired*". In this phase, the decision variables with indices in I_{p} are used to create purity margin enabling those with indices in I_{a} to decrease the auxiliary cost. It is crucial to note that since the auxiliary cost depends only on the decision variables with indices in I_{a} [see (30)–(32)], the auxiliary cost remains unchanged during the purity margin's creation phases.

5.1. Robustness against uncertainties

In order to make the controlled system robust against uncertainties (equivalent void fraction, isotherm coefficients, ...), an integrator effect has to be introduced. This is done using the purity margin η. Note that under free-uncertainty context and for sufficiently long prediction horizon, the property $J_{\text{pur}}^{\text{inv}} \leqslant 0$ is invariant. In other words, if $J_{\text{pur}}^{\text{inv}}$ changes its sign from negative to positive, one must deduce that there are errors on the parameters used in the prediction. In such a case, the purity margin must be increased in order to guarantee the purity requirements achievement. That is why whatever is the active configuration ($C(t_k, U^k) \in \mathscr{A}_\eta^{\text{ad}}$ or not) the following updating rule is used for η_k:

$$\begin{aligned}&\text{if } (J_{\text{pur}}^{\text{inv}}(k) > 0 \text{ and } J_{\text{pur}}^{\text{inv}}(k-1) \leqslant 0) \text{ then}\\ &\eta_k \leftarrow \eta_k + \delta_\eta\\ &\text{Else}\\ &\eta_k \leftarrow \max\{\eta_{\min}, \gamma\eta_{k-1}\}; \quad \gamma < 1\\ &\text{Endif}\end{aligned} \tag{37}$$

Where $\eta_{\min}$ is a minimal purity margin that is used in the nominal configuration.

5.2. Some computational issues

In the present section, some computational issues concerning the feedback algorithm presented in Section 5 are clarified. In particular, the role and the updating rules of the trust region parameters α_i^k are explained.

The solution of (27) [respectively (33)] is based on a qth order approximation of the cost function J_{pur} [respectively $J_{\text{pur}}^{\text{inv}}$] as a function of U_i^k. This approximation needs q evaluations and is made on a so called trust region defined by the present value of α_i^k, namely

$$[U_i^k - \alpha_i^k\delta_i, U_i^k + \alpha_i^k\delta_i] \cap \mathbb{U}_i(U^k) \tag{38}$$

where $\delta_i > 0$ is some fixed step value and $\mathbb{U}_i(U^k)$ is the admissible region of the ith component that is compatible with $\mathbb{U}$.

Based on the use of this approximation, a candidate solution $\widehat{U}^{k+1}$ is obtained. If $J_{\text{pur}}(\widehat{U}^{k+1}) < J_{\text{pur}}(U^k)$ [respectively $J_{\text{pur}}^{\text{inv}}(\widehat{U}^{k+1}) \leqslant J_{\text{pur}}^{\text{inv}}(U^k)$], then the solution is adopted and the trust region is enlarged

$$U^{k+1} \leftarrow \widehat{U}^{k+1}, \quad \alpha_i^k \leftarrow \beta^+\alpha_i^k, \quad \beta^+ > 1 \tag{39}$$

otherwise, $U^{k+1} = U^k$ and the following updating rule is used to reduce the trust region:

$$\alpha_i^k \leftarrow \max\{\beta^-\alpha_i^k, \alpha_{\min}\}, \quad \beta^- < 1 \tag{40}$$

where $\alpha_{\min} > 0$ is used to prevent the "*collapse*" of α_i^k when the optimal solution is reached. This maintains the reactivity of the control algorithm.

6. Illustrative simulations

First of all, it is worth noting that the feedback scheme proposed in this paper is independent of the particular structure of the simulator. The latter is invoked by the feedback algorithm as a black box prediction tool that gives for some control profile the corresponding future evolution.

In this section, some illustrative scenario are simulated in order to assess the efficiency of the proposed strategy. The controller efficiency is tested using two different SMB's with respectively medium and high separation capacities.

6.1. Medium separation SMB

6.1.1. The simulation model

The particular model used in this section is based on the use of a cascade of perfectly agitated reactors to model each single column. The number of columns in each section is equal to 5, each column is modelled by 4 reactors in series. Therefore, the total number of reactors used to model the whole SMB is equal to $n_c = 80$. A langmuir nonlinear isotherm is used with constants $K_1 = 0.56$ (cm^3/g) and $K_2 = 0.2$ (cm^3/g) with saturation loading capacities $qm_1 = qm_2 = 1$ g/cm^3. Both feed concentrations are equal to 0.05 g/cm^3. The column diameter, length and void fraction used in the simulations are:

$$D = 3.68 \text{ cm}, \quad L = 53.6 \text{ cm}, \quad \epsilon = 0.45$$

The nominal flow rates are those appearing at the initial instant on Fig. 3. The switching time is 30 s.

Consequently, a system of 160 first order ODE's is obtained that is solved by LSODA implemented in FORTRAN 90 code.

6.1.2. The controller parameters

The saturation level $U_i^{\max} = 0.15$ cm^3 s^{-1} on the flow rates is used. The number of iterations per switching period $N = 1$ is applied in order to carry on to its limit the distributed in time optimization principle. The basic incremental values

$$\delta = (0.005, 0.005, 0.005, 0.0025, 2.5)^{\text{T}}$$

are used in (38). In (37), updating η_k is done using $\delta_\eta = 0.005$, $\eta_{\min} = 0.001$ and $\gamma = 0.95$. Finally, the pair $(\beta^+, \beta^-) = (2, 0.5)$ is used in (39) and (40) to update the trust region coefficient $\alpha_{i.}$

6.1.3. Simulations

Two different scenario have been simulated for this medium separation SMB.

6.1.3.1. Scenario 1 (Figs. 3–5): startup and step change in the desired purities. Efficiency related auxiliary cost: $J_\alpha := \frac{Q_D}{Q_F}$. The system is initially with uniform concentra-

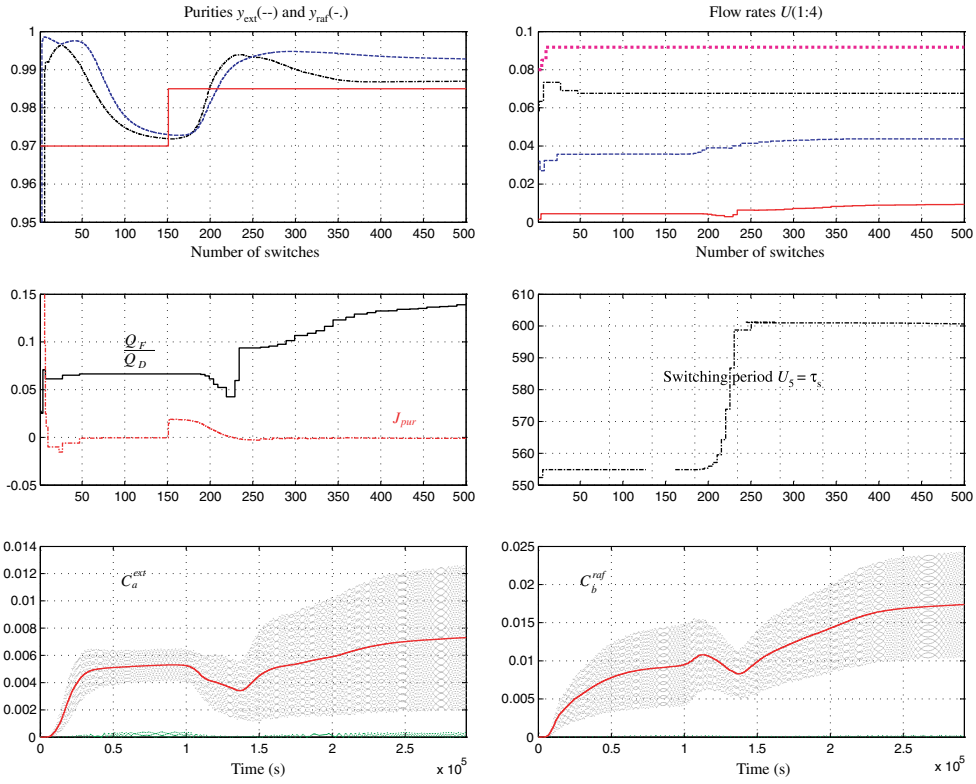

Fig. 3. Response of the controlled SMB to a step change of the desired purities $y_d \cdot y_d$ changes at $k = 150$ from (0.97, 0.97) to (0.99, 0.99).

tions close to 0 ($C \equiv 0.001$ everywhere). A first step $y_d = (0.97, 0.97)$ is applied and after 150 switching periods, a step change is applied to require purities $y_d = (0.985, 0.985)$. Fig. 3 shows plots related to this experiment. The purities evolution and the flow rates are shown on the two top plots. Note in particular that the initial values of the flow rates was not appropriate. This can be particularly seen on the J_{pur} evolution (plot(2, 1) of Fig. 3) where it can be observed that the initial value of J_{pur} is highly positive indicating that the mean steady state regime corresponding to the initial values of the flow rates and the switching time (the control U) does not satisfy the purity requirement $y_d = (0.97, 0.97)$. The auxiliary cost function J_a used in this experiment is $J_a = Q_D/Q_F$. The evolution of the efficiency ratio Q_F/Q_D is shown on the plot(2, 1) of Fig. 3. This shows how the feedback algorithm increases this ratio as soon as the purity requirements are guaranteed. This ratio may however decrease on transient periods where these purities are not guaranteed, for instance in the transient following the step change in the purities (between $k = 150$ and $k = 230$), and then increases as soon as the closed-loop retrieves guarantee of purities achievement. The two bottom figures also show the role of the yield related weighting term in (22) and (23) in increasing the corresponding yield. Note that the two bottom figures show the cyclic behavior as well as the corresponding mean values over the switching period.

The evolution of the trust region parameters $(\alpha_i)_{i=1}^5$ is depicted on Fig. 4. From this figure, it can be inferred that before the step change at $k = 150$, a local minimum has been reached since all the trust region parameters tend to 0 since no better solution can be found in the neighborhood of the one already found. As soon as a step change in the desired purities is applied, these parameters"*wake up*" to modify the control value in order to meet the new requirements.

Finally, Fig. 5 shows a zoom on the evolution of the purity related cost functions J_{pur} and J_{pur}^{inv}. Note first that J_{pur} reaches the negative values before J_{pur}^{inv} since it is exclusively concerned by the final mean steady values of the purities while J_{pur}^{inv} needs the whole purities from the current instant to *infinity*" to satisfy the purity requirements. The chattering behaviour schematically depicted in Fig. 2 can be clearly observed where J_{pur} (and J_{pur}^{inv}) alternatively decreases and increases according to the nature of the decision variable being optimized leading to either purity margin creation or to decreasing the auxiliary cost (see Fig. 2).

6.1.3.2. Scenario 2 (Fig. 6): startup and unmeasured step change in the void fraction. Robustness against parameter uncertainties. Efficiency related auxiliary cost: $J_a := \frac{Q_D}{Q_F}$. The first 150 switching periods are the same as those of the preceding scenario. At $k = 150$, instead of a step change in the required purities, an unmeasured

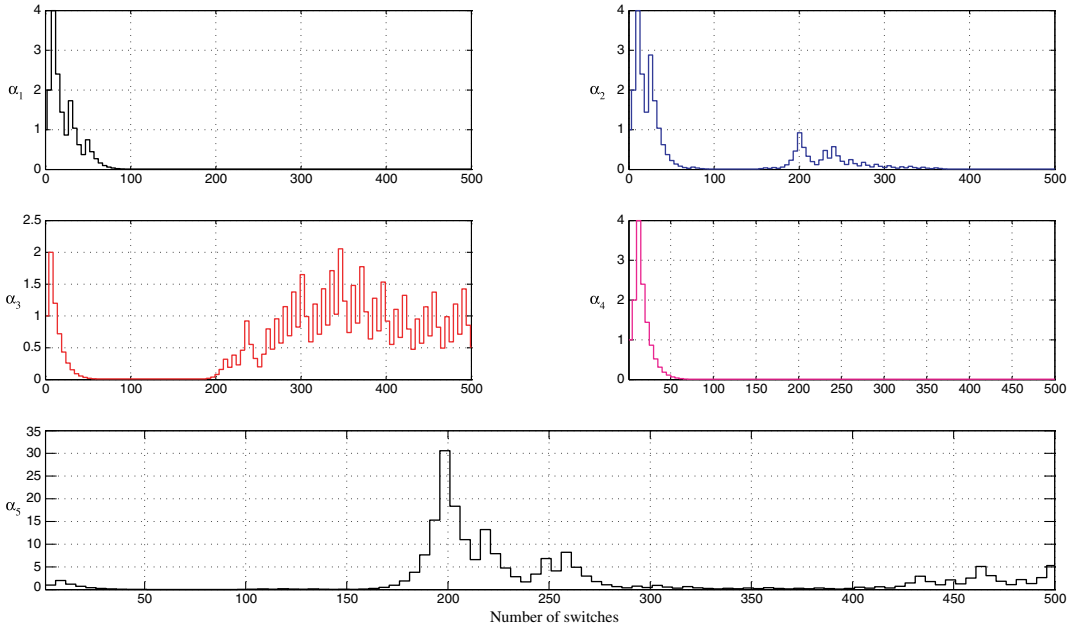

Fig. 4. Evolution of the trust region parameters α_i during the experiment depicted in Fig. 3.

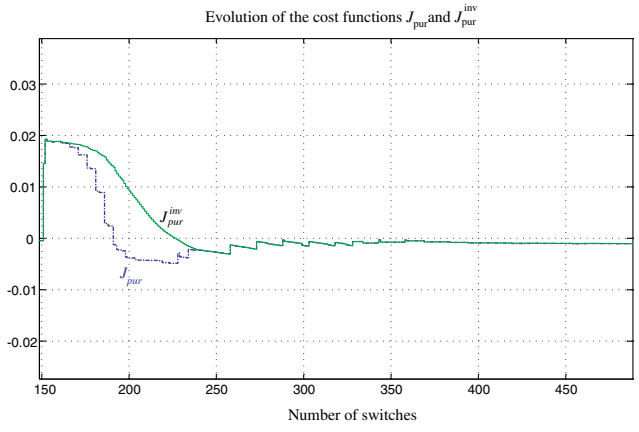

Fig. 5. Zoom on the cost functions evolution after the step change in the desired purity y_d.

(−10%) step change in the void fraction ϵ is applied in order to test the robustness of the closed-loop system to parameter uncertainties. Plot(1,1) of Fig. 6 also shows the behaviour of the system if open-loop control is used after $k = 150$. This enables to evaluate the effect of the parameter uncertainties on the purities that would have been obtained in the absence of feedback. Note that the controller reacts in order to maintain the required purities in spite of the error in the parameter it uses. On the other hand, the auxiliary efficiency criterion as well as the yield is still increased despite the error on the key parameter ϵ. Note however that this increase is no more monotonic since the condition $J_{pur} \leqslant 0$ is no more invariant and the controller swings between periods where the primary purity requirements are looked for and periods where the auxiliary cost function is decreased. This can be viewed on the plot (2, 1) of Fig. 6 where it can be observed that J_{pur} oscillates around 0. Comparable results were obtained when simulating the system reaction to uncertainty of +15% on the Langmuir coefficients K_1 and K_2. Simulations were not reported for lake of space.

6.2. High separation nonlinear SMB

6.2.1. The simulation model

In this section, a high purity dedicated nonlinear SMB is used. Finite difference scheme is used to solve the system convection diffusion PDE's. Here, the Langmuir coefficients belong to a difficult chromatographic separation task ($K_1 = 2\ \mathrm{cm^3/g}$, $K_2 = 1.5\ \mathrm{cm^3/g}$), the saturation level capacities $q_{m_1} = q_{m_2} = 1\ \mathrm{g/cm^3}$ are taken. Both feed concentrations are equal to $0.005\ \mathrm{g/cm^3}$. Two columns per section have been used with 20 nodes per columns for the finite difference scheme. This leads to a system with 320 state variables. The SMB parameters are the following

$$D = 5\ \mathrm{cm}, \quad L = 50\ \mathrm{cm}, \quad \epsilon = 0.4$$

The nominal flow rates are taken equal to the central values with respect to the minimal and maximal values defined hereafter. The nominal switching time is 30 s.

6.3. The controller parameters

The values of $U_{\min}$ and $U_{\max}$ have been taken as follows:

$$U_{\max} = (117\ 82\ 6\ 128\ \mathrm{cm^3\ s^{-1}}\ 33\ \mathrm{s})$$

$$U_{\min} = (95\ 68\ 5\ 105\ \mathrm{cm^3\ s^{-1}} 27\ \mathrm{s})$$

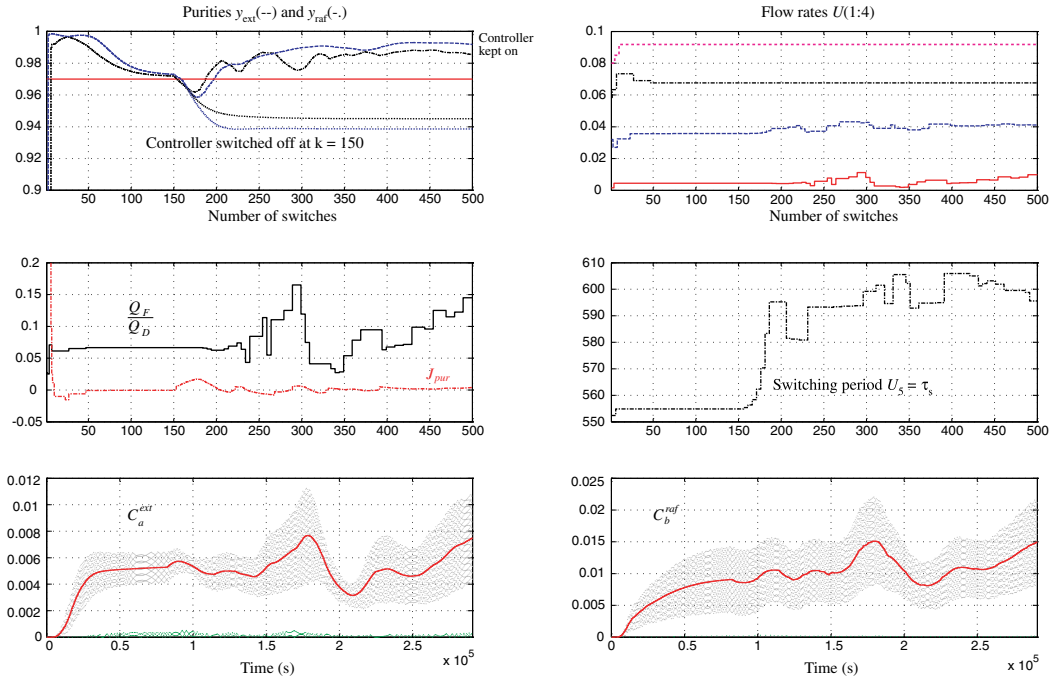

Fig. 6. Response of the controlled/uncontrolled SMB to a unmeasured −10% step change of the void fraction ε.

the values of the $\delta_i's$ was taken equal to 1% of the central value for each U_i. The parameters $\beta^+ = 1.8$, $\beta^- = 0.7$, $\eta_{\min} = 0.001$ and $\gamma = 0.95$ have been used.

6.3.1. The simulations

Three scenario have been tested in order to assess the basic claims of this paper:

(1) Constant desired purities with changes in the fired auxiliary cost (Fig. 7).

The aim here is to assess the flexibility of the proposed scheme and its reactivity to sudden changes in the auxiliary cost function. The desired high purities are fixed at $y_d = (0.992, 0.997)$. The auxiliary cost is $J_a = Q_D/Q_{ext}$ over the first 500 switches (Phase 1 on Fig. 7), $J_a = Q_F/Q_{ext}$ during the next 500 switches (Phase 2 on Fig. 7) while the maximum flow rate cost $J_a = Q_D + Q_F$ is used during the last phase (Phase 3 on Fig. 7).Note how the controller takes into account the sudden changes

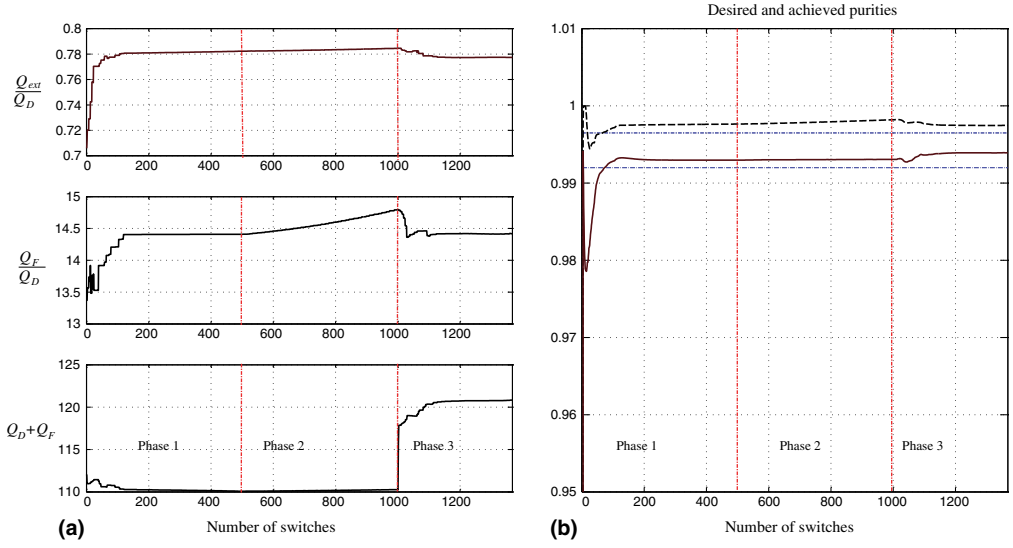

Fig. 7. Scenario 1, High separation SMB. (a) The purities and their set point $y_d = (0.992, 0.997)$. (b) The different cost functions fired at different instants during the scenario. Note how the controller takes into account the sudden changes in the fired auxiliary cost and increases appropriately the corresponding value while keeping the purities above the required set-points.

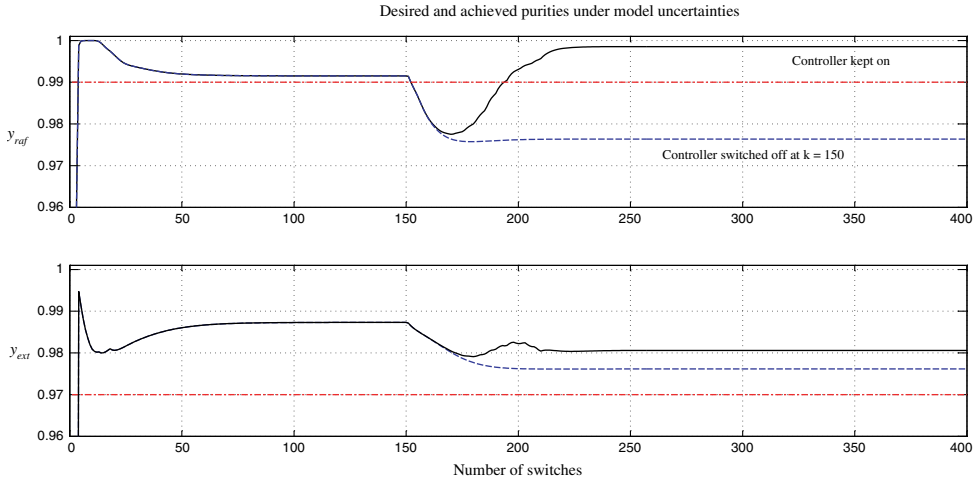

Fig. 8. Behaviour of the closed loop system (continuous line) and the system with the controller switched off after the 150th switch (dotted line) in the presence of +1.8% unmeasured step change of the Langmuir coefficients.

in the fired auxiliary cost and increases appropriately the corresponding value while keeping the purities above the required set-points.

(2) Robustness against model uncertainties (Fig. 8). In this scenario, a small error (+1.8%) on both Langmuir coefficients K_1 and K_2 is introduced, namely, the true system is more sensitive than the one used by the controller. Fig. 8 shows how the closed loop system retrieves the specified purities. The plots show the response that would be obtained if the controller was switched off just after the 150th switch where the step on model error is introduced. This shows the high sensitivity of such high separation SMB to model uncertainties and suggests to use some on-line identification scheme in conjunction with the proposed control strategy. Note that during this simulation, the related auxiliary cost function $J_a = \frac{Q_D}{Q_{ext}}$ is used.

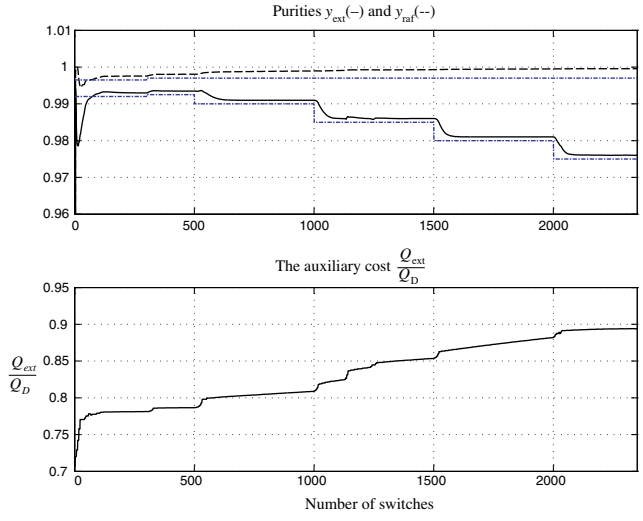

Fig. 9. Response of the controlled SMB to different references.

(3) Successive setpoint changes in the desired purities.Finally, Fig. 9 shows how the controller improves the auxiliary cost when decreasing steps are applied on the one of the desired purities.

7. Conclusion

In this paper, a nonlinear model predictive control is proposed for the control of a simulated moving bed with highly nonlinear isotherm. The key feature of the proposed scheme is that the optimization is distributed on the plant life time according to the available computation time. Furthermore, several performance indexes may be easily handled and online changed according to the production scheduling context. Simulations show good robustness of the closed-loop system against uncertainties on the system parameters (void fraction, isotherm coefficients). No a priori knowledge of the optimal profile is needed since the feedback scheme is not based on regulation around some pre-computed trajectories. However, any such knowledge may be easily included in the feedback initialization to improve its performance. The feedback scheme may be applied to a wide class of processes since only the "*black box*" prediction of the future behavior is needed for the feedback implementation. Note however that for highly sensitive SMB, the proposed control scheme (as any other one) has to be coupled with an on-line parameter identification. The robustness of any feedback approach with such systems reaches its limit.

References

[1] H. Schramm, S. Gruner, A. Kienle, Optimal operation of simulated moving bed chromatographic processes by means of

simple feedback control, Journal of Chromatography A (1006) (2003) 3–13.
[2] E. Kloppenburg, E.D. Gilles, Automatic control of the simulated moving bed process for C_8 aromatics separation using asymptotically exact input/output linearization, Journal of Process Control 9 (1999) 41–50.
[3] S. Abel, G. Erdem, M. Mazzotti, M. Morari, M. Morbidelli, Optimizing control of simulated moving beds-linear isotherm, Journal of Chromatography A (1033) (2003) 229–239.
[4] N. Seshatre, J.H. Lee, Repetitive model predictive control applied to a simulated moving bed chromatography system, Computers and Chemical Engineering 24 (2000) 1127–1133.
[5] U.K. Klatt, F. Hanisch, G. Dunnebier, Model-based control of a simulated moving bed chromatographic process for the separation of fructose and glucose, Journal of Process Control 12 (2002) 103–219.
[6] A. Toumi, S. Engell, Optimization-based control of a reactive simulated moving bed process for glucose isomerization, Chemical Engineering Science 43 (14) (2004) 3895–3907.
[7] D.Q. Mayne, J.B. Rawlings, C.V. Rao, P.O.M. Scokaert, Constrained model predictive control: Stability and optimality, Automatica 36 (2000) 789–814.
[8] M. Mangold, G. Lauschke, J. Schaffner, M. Zeitz, E.-D. Gilles, State and parameter estimation for adsorption columns by nonlinear distributed parameter state observers, Journal of Process Control 4 (3) (1994) 163–172.
[9] M. Alamir, J.P. Corriou, Nonlinear receding horizon state estimation for dispersive adsorption columns with nonlinear isotherm, Journal of Process Control 13 (6) (2003) 517–523.
[10] L. Robertson, J.B. Rawlings, A moving horizon-based approach for least-squares estimation, AIChE 42 (8) (1996) 2209–2224.
[11] J.P. Corriou, M. Alamir, A hybrid nonlinear state observer for concentration profiles reconstruction in nonlinear simulated moving beds, Journal of Process Control, in press, doi:10.1016/j.jprocont.2005.07.002.